



**Enhancement of fluorescence and photostability of
luminescent radicals by quadruple addition of phenyl groups**

Journal:	<i>Journal of Materials Chemistry C</i>
Manuscript ID	TC-ART-07-2022-003132.R1
Article Type:	Paper
Date Submitted by the Author:	26-Aug-2022
Complete List of Authors:	Mattiello, Sara; University of Milano-Bicocca, Materials Science Hattori, Yohei; Ryukoku University - Seta Campus, Materials Chemistry Course, Faculty of Advanced Science and Technology Kitajima, Ryota; Ryukoku University - Seta Campus, Materials Chemistry Course, Faculty of Advanced Science and Technology Matsuoka, Ryota; Institute for Molecular Science, Department of Life and Coordination-Complex Molecular Science Kusamoto, Tetsuro; Institute for Molecular Science, Department of Life and Coordination-Complex Molecular Science Uchida, Kingo; Ryukoku University, Department of Materials Chemistry Beverina, Luca; University of Milan-Bicocca, Materials Science

ARTICLE

Enhancement of fluorescence and photostability of luminescent radicals by quadruple addition of phenyl groups

Sara Mattiello ^{*a} Yohei Hattori ^{*b} Ryota Kitajima ^b Ryota Matsuoka ^{c,d} Tetsuro Kusamoto ^{c,d,e} Kingo Uchida ^b and Luca Beverina ^a

Received 00th January 20xx,
Accepted 00th January 20xx

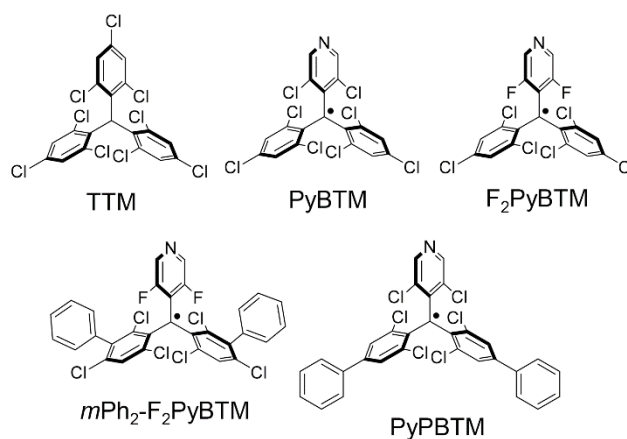
DOI: 10.1039/x0xx00000x

Quadruple addition of phenyl groups to a diphenylpyridylmethane skeleton was achieved. The derived (3,5-difluoro-4-pyridyl)bis(2,6-dichloro-3,4-diphenylphenyl)methyl radical (Ph₄-F₂PyBTM) displayed superior luminescent properties to the previously reported organic diphenylpyridylmethyl radicals in various organic solutions at room temperature, and it reached 33% photoluminescence quantum efficiency in PMMA film. With the introduction of methoxy groups, quadruple adduct (MeOPh)₄-F₂PyBTM and triple adduct (MeOPh)₃-F₂PyBTM were isolated. The excited state of these radicals showed an intramolecular charge transfer character and efficient fluorescence only in nonpolar solvents. The radicals retained not only persistency at the ground state but also durability under photoirradiation, with a 6 to 14 fold improved photostability with respect to the original PyBTM.

Introduction

Stable luminescent radicals, which show fluorescence associated with the transition from the doublet lowest excited state to the doublet ground state, have been actively developed recently.¹ Due to the absence of quenching via the triplet state seen in the closed-shell luminescent molecules, they are suitable luminophores for electroluminescent devices.² Their unique luminescence also allows other possible applications, such as use in heavy atom environments³ and magnetoluminescence.⁴

The biggest concern in using a luminescent radical has been its stability. We reported that the introduction of a pyridyl group instead of a phenyl group in the polychlorotriphenylmethyl radical, the most common stable luminescent radical, largely improved the stability of the radical under photoirradiation.⁵ Compared with tris(2,4,6-trichlorophenyl)methyl radical (TTM),⁶ (3,5-dichloro-4-pyridyl)bis(2,4,6-trichlorophenyl)methyl radical (PyBTM, Scheme 1) showed *ca.* 70 times higher photostability in dichloromethane. The photostability of PyBTM can be further improved by the introduction of additional pyridyl groups⁷ or Au^I complexation.⁸



Scheme 1 Structures of TTM and PyBTM derivatives.

Replacing chlorine with fluorine on the pyridine leads to a (3,5-difluoro-4-pyridyl)bis(2,4,6-trichlorophenyl)methyl radical (F₂PyBTM) having higher fluorescence efficiency but lower photostability than PyBTM.⁹ The introduction of two phenyl rings at the *meta* position with respect to the radical site (α -carbon) yields a (3,5-difluoro-4-pyridyl)bis(3-phenyl-2,4,6-trichlorophenyl)methyl radical (*m*Ph₂-F₂PyBTM) with higher photostability but lower fluorescence efficiency than PyBTM.¹⁰ Recently, we made the first report on the use of a radical as an organic luminophore for a transparent luminescent solar concentrator (LSC).¹¹ A PyBTM derivative having phenyl groups *para* to the α -carbon: (3,5-dichloro-4-pyridyl)bis(2,6-dichloro-4-phenylphenyl)methyl radical (PyPBTM) provided a particularly suitable combination of emission efficiency and separation between absorption and emission spectra. The selective substitution of the 4-chloro group of α H-PyBTM (precursor of PyBTM) was achieved with the development of

^a Department of Materials Science, University of Milano-Bicocca, Via R. Cozzi 55, 20126 Milano, Italy. E-mail: sara.mattiello@unimib.it

^b Materials Chemistry Course, Faculty of Advanced Science and Technology, Ryukoku University, Seta, Otsu, Shiga 520-2194, Japan. E-mail: hattori@rins.ryukoku.ac.jp

^c Department of Life and Coordination-Complex Molecular Science, Institute for Molecular Science, 5-1, Higashi-yama, Myodai-ji, Okazaki, Aichi 444-8787, Japan.

^d SOKENDAI (The Graduate University for Advanced Studies), Shonan Village, Hayama, Kanagawa 240-0193, Japan.

^e JST-PRESTO, 4-1-8, Honcho, Kawaguchi, Saitama 332-0012, Japan.

† Electronic Supplementary Information (ESI) available: See DOI: 10.1039/x0xx00000x

the Suzuki-Miyaura coupling reaction with micellar catalysis (Micellar Suzuki-Miyaura MSM).¹²

Here, we applied the MSM protocol and succeeded in synthesizing new diphenylpyridylmethyl radical derivatives having phenyl groups both *para* and *meta* to the α -carbon. Triarylmethyl radicals in this substitution form have not been previously reported. We report a (3,5-difluoro-4-pyridyl)bis(2,6-dichloro-3,4-diphenylphenyl)methyl radical (Ph₄-F₂PyBTM, **1**) and related compounds (**2**, **3**, Scheme 2) as well as their improved fluorescence quantum yields and photostability.

The radicals (MeOPh)₄-F₂PyBTM (**2**) and (MeOPh)₃-F₂PyBTM (**3**) have electron-rich *p*-methoxyphenyl groups. Polychlorotriphenylmethyl radicals with electron donors such as carbazoles^{2e,13} or triphenylamines^{13d,14} have been reported to show high fluorescence quantum yields. Recently, improved photostability by adding donors to radicals has also been reported.^{2ef,13d,15} We studied whether methoxy groups could serve as such donors to improve fluorescence efficiency and photostability.

Results and discussion

The precursor of Ph₄-F₂PyBTM (**1**): α H-Ph₄-F₂PyBTM (**1H**) was synthesized by Suzuki-Miyaura coupling between phenylboronic acid and (3,5-difluoro-4-pyridyl)bis(3-bromo-2,4,6-trichlorophenyl)methane (α H-*m*Br₂-F₂PyBTM), the compound we previously used to prepare *m*Ph₂-F₂PyBTM by Migita-Kosugi-Stille coupling.¹⁰ Probably two bromine atoms at the *meta*-positions were first substituted and then two chlorine atoms at *para*-positions were substituted by phenyl groups. The substitution at adjacent bromo and chloro groups show the powerful nature of this reaction. No such result was possible by performing the reaction under standard, organic solvent-based conditions. The compound **1H** was purified by column

chromatography and GPC separation (see Supporting Information). A compound with three phenyl rings, α H-Ph₃-F₂PyBTM was observed as a by-product, but we could not isolate it as a pure compound.

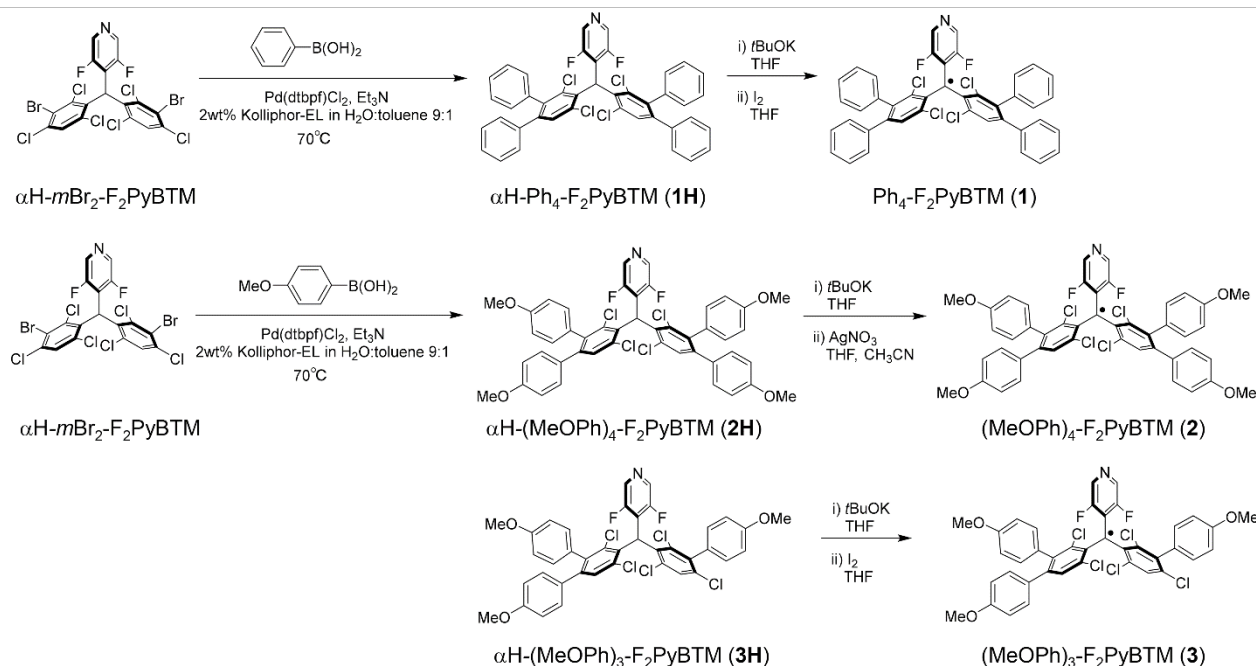
The precursor of (MeOPh)₄-F₂PyBTM (**2**): α H-(MeOPh)₄-F₂PyBTM (**2H**) and the precursor of (MeOPh)₃-F₂PyBTM (**3**): α H-(MeOPh)₃-F₂PyBTM (**3H**) were synthesized by Suzuki-Miyaura coupling between 4-methoxyphenylboronic acid and α H-*m*Br₂-F₂PyBTM. Thanks to the methoxy group, these compounds were relatively easily separated.

The radicals **1**, **2**, and **3** were prepared by deprotonation and oxidation of the corresponding precursors. All radicals were stable under ambient conditions. Cyclohexane solutions showed ESR signals for the spin $S = 1/2$ (Fig. 1a).

The electronic structures of the radicals were calculated by DFT at the UB3LYP/6-31G(d) level (Fig. 1b, Table S1). The lowest energy electron transition of each radical is expected to consist of the β -HOMO \rightarrow β -LUMO transition, which is typical for polychlorotriarylmethyl radicals.^{2bcef,3,5,7} The β -LUMOs are centered on α -carbon atoms and delocalized on bonded pyridyl and two phenyl rings. The β -HOMOs are distributed on *o*-diphenylphenyl groups, which are the most electron-rich part of these molecules. Energy levels of the frontier orbitals of **2** and **3** were slightly raised by the electron-rich methoxy groups.

The absorption and emission spectra of **1**, **2**, and **3** in cyclohexane are shown in Fig. 1c. Weak absorption between 15,000 and 22,000 cm⁻¹ is derived from transitions of the β -spin electrons to the β -LUMO. The radicals with methoxy groups (**2** and **3**) indicate lower energy absorption since they have higher occupied β -spin orbitals. Stronger absorption around 24,000–28,000 cm⁻¹ is mainly attributed to the transition of the α -HOMO electron to the α -spin unoccupied orbitals. These are characteristic absorption bands of triarylmethyl radicals, and they are confirmed by TD-DFT calculations (Table S2). The short-

Scheme 2 Synthetic scheme of **1**, **2**, and **3**.



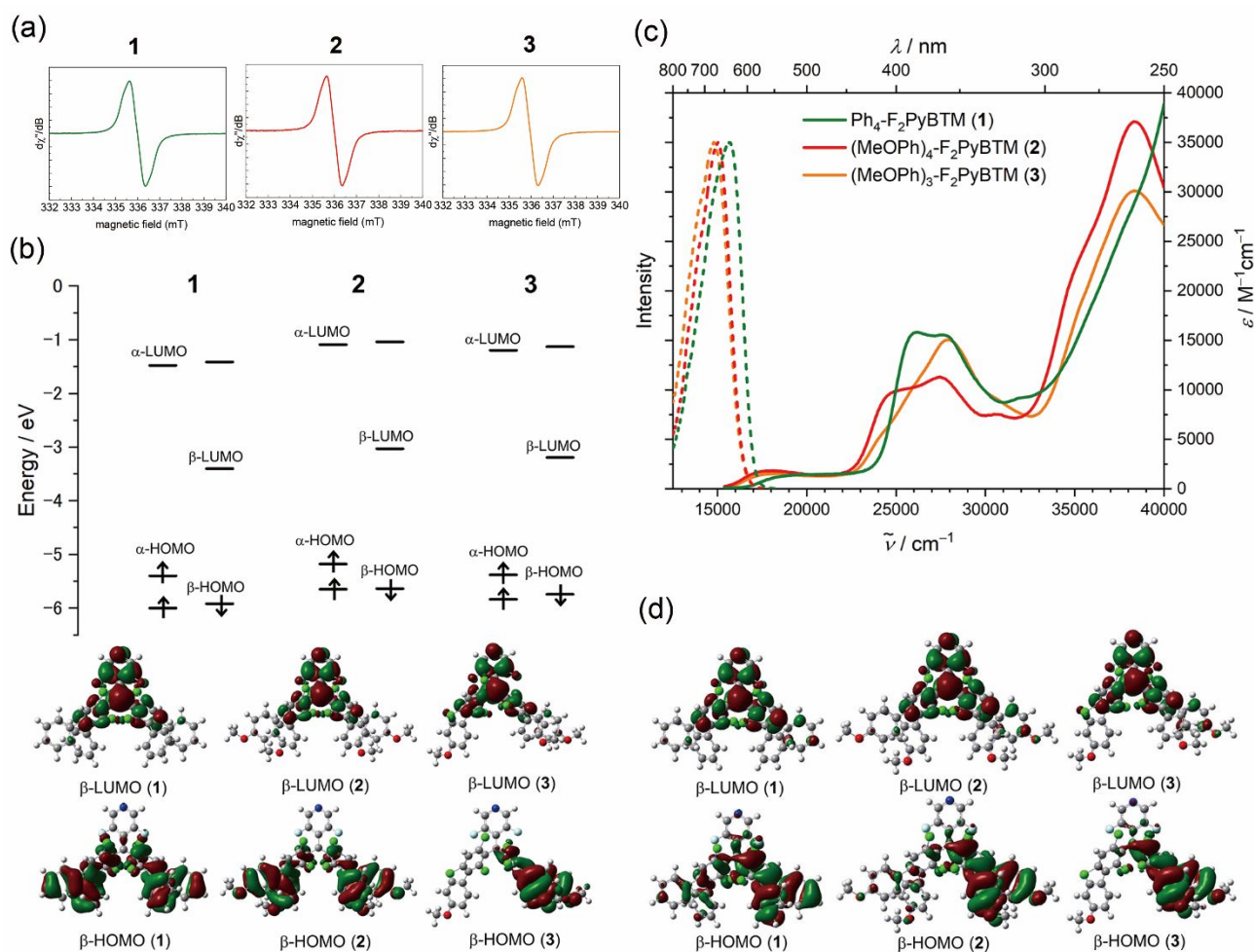


Fig. 1 (a) EPR spectra of **1**, **2**, and **3** in cyclohexane (ca. 4.4). The g factors of the radicals were $g = 2.003$. The concentrations of the ESR solutions were ca. 44, 32, 65 μM , respectively, and the double integral of the signal was 34: 22: 53. The signal per concentration was 0.77: 0.69: 0.82, which is within the error range. (b) Energies of frontier orbitals and shapes of the β -HOMO and β -LUMO of **1**, **2**, and **3** at D_0 ground state optimized using UB3LYP/6-31G(d). (c) Absorption (solid line) and emission (broken line) spectra of **1** (green), **2** (red), and **3** (orange). (d) Shapes of the β -HOMO and β -LUMO of **1**, **2**, and **3** at D_1 excited state optimized using UM06-2X/6-31G(d).

wavelength absorption between 35,000 and 40,000 cm^{-1} is stronger than that of the previously reported PyBTM derivatives due to the increased number of phenyl rings.

To consider the fluorescence from the D_1 lowest excited state, the molecular structures at the D_1 excited state were optimized using UM06-2X/6-31G(d), since this was reported to demonstrate better agreement with the emission for triarylmethyl radicals.¹⁶ The shapes of the β -LUMOs were similar to the ground states, while the β -HOMOs were localized on one side of the *o*-diphenylphenyl group (Fig. 1d). The symmetry of the dihedral angles of **1** and **2** (Table S1) was broken, and the *p*-phenyl group under β -HOMO conjugated more strongly with the dichlorophenyl group with a smaller dihedral angle (Table S3, 4). As a result, the shapes of the β -HOMOs of **2** and **3** were similar. In both the ground (D_0) and lowest excited (D_1) states, the electronic structures of these radicals are classified as donor- π -acceptor (D- π -A)-type,¹⁷ in which the added *o*-diphenylphenyl group works as a donor and the radical (unpaired orbital) works as an acceptor.

The emission maxima of **1**, **2**, and **3** in cyclohexane were 639, 666, and 676 nm, respectively. The order of emission maxima was similar to the order expected by TD-DFT calculations at the D_1 state in various methods (Table S5). Use of UBMK/6-31G(d) gave a relatively good expectation of the emission wavelengths, as reported for the calculations of other triarylmethyl radicals.¹⁶ The longer wavelengths of emission for the radicals with methoxy groups are attributed to the higher energies of β -HOMO orbitals.

Table 1 Fluorescence quantum yields and emission maxima of **1**, **2**, and **3**.

	1	2	3
Cyclohexane	6% (639 nm)	17% (666 nm)	15% (676 nm)
Toluene	9% (641 nm)	19% (718 nm)	11% (725 nm)
Chloroform	13% (643 nm)	2% (745 nm)	1% (769 nm)
Dichloromethane	11% (653 nm)	0.3% (780 nm)	0.3% (815 nm)
Acetone	11% (655 nm)	0%	0%

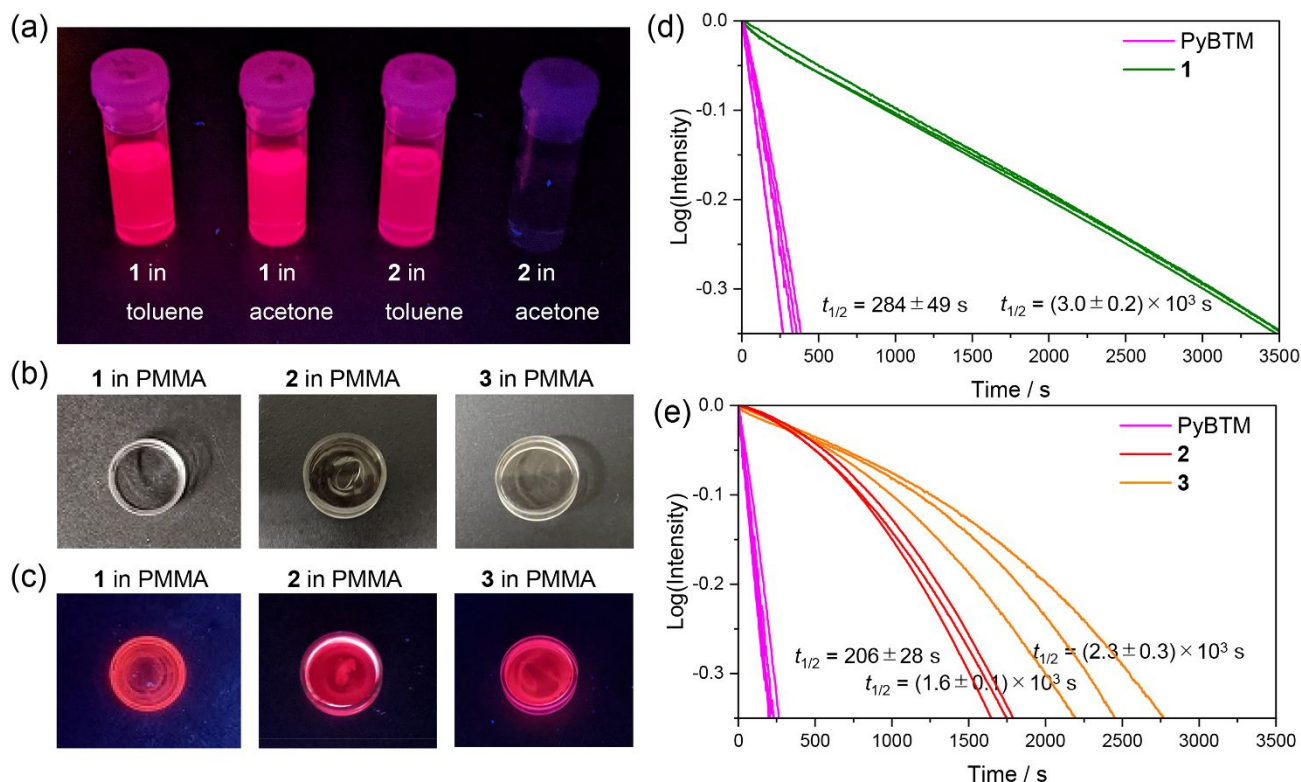


Fig. 2 (a) Picture of **1** in toluene, **1** in acetone, **2** in toluene, and **2** in acetone under UV ($\lambda = 365$ nm) light. (b) Picture of a PMMA film containing **1**, **2**, and **3** in a Petri dish under white light. (c) Picture of a PMMA film containing **1**, **2**, and **3** in a Petri dish under UV ($\lambda = 365$ nm) light. (d) Plots showing emission decay of **1** and PyBTM in dichloromethane under continuous excitation with light at $\lambda_{\text{ex}} = 370$ nm \pm 10 nm. (e) Plots showing emission decay of **2**, **3**, and PyBTM in cyclohexane under continuous excitation with light at $\lambda_{\text{ex}} = 370$ nm \pm 10 nm.

The fluorescence spectra and fluorescence quantum yields (Φ_f) upon excitation at $\lambda_{\text{ex}} = 370$ nm in various solvents were measured (Table 1). Fluorescence lifetimes and photophysical parameters are shown in Table S6. The fluorescence of the radicals with methoxy groups indicated quenching of luminescence in polar solvents, with the effect becoming more evident at increased polarity in this series: chloroform, dichloromethane, acetone (Fig. 2a). Polarity also red shifts the emission. Such a bathochromic shift is explained by the relaxation of the polar D_1 state by reorganization of the polar solvent molecules, and the quenching is the fast deactivation of the low-lying excited state. The bathochromic shift was slightly larger in **3** than in **2**, because the β -HOMO of **3** was more localized on one side of the *o*-(dimethoxyphenyl)phenyl group (Fig. 1d). Probably this is why **3** had a shorter lifetime (Table S6) and lower quantum yield (Table 1) in toluene and chloroform than **2**. Quenching in the polar solvent was reported in furan or thiophene ring-attached F_2 PyBTM (*mFu*₂- F_2 PyBTM and *mTh*₂- F_2 PyBTM)¹⁰ and other donor- π -radical systems.^{13,18}

In contrast, **1** was fluorescent in both nonpolar and polar organic solvents. Indeed, **1** showed the strongest fluorescence in chloroform among the organic solvents, similarly to PyBTM⁵ and F_2 PyBTM.⁹ Remarkably, **1** is also brightly fluorescent in toluene, where the aforementioned related radicals are efficiently quenched.⁵ Molecular interaction such as π - π stacking between excited radical and toluene solvent was

probably prevented by four phenyl groups. Emission maxima shifted slightly to longer wavelengths with increasing solvent polarity. However, these shifts were much smaller than those observed for **2** and **3**. This means that **1** has a locally excited character rather than an intramolecular charge transfer (ICT) character. These phenomena were also reported in D- π -A-type radicals with a diminished donor character.^{13c,15} The lack of electron-donation from the methoxy group caused the difference in the D_1 excited state properties.

PyBTM derivatives are superior radicals in their photostability, showing highly efficient ($\Phi_f = 89\%$) luminescence in doped crystals;^{4a} however, they suffer from their low fluorescence efficiency in solutions.⁵ The fluorescence quantum yield of F_2 PyBTM (6% in chloroform) was enhanced by Au^I coordination to the nitrogen atom,^{8bc} but no pure organic PyBTM derivative has achieved Φ_f above 10% in organic solvents. The fluorescence quantum yields of 13% of **1** in chloroform and 19% of **2** in toluene are the largest ever reported for PyBTM-like derivatives. The quantum yield of 15% of **3** in cyclohexane is also a relatively large value, hinting at the possibility of avoiding the fourth addition of the benzene ring. Since their fluorescence lifetimes ($\tau = 13$ -15 ns at most, Table S6) were not so much longer than that of F_2 PyBTM ($\tau = 12.5$ ns in chloroform),⁹ the fluorescence enhancement is mainly attributed to the increased rates of fluorescence transition (k_f , Table S6). A similar phenomenon was seen in locally excited

gold complexes as the breaking of forbidden transitions due to three-fold symmetry.⁸ In donor-acceptor radicals, the phenomenon is theoretically explained as intensity borrowing effects.^{2f,19}

Considering its application in devices such as OLEDs and LSCs, fluorescence in solid film is important. We made a poly(methyl methacrylate) (PMMA) film containing **1**, **2**, and **3** (Fig. 2b). The fluorescence quantum yield of the film containing **1** was 33%, which was the largest value of the PyBTM derivatives in PMMA film (Fig. 2c). Rigid polymer chains are thought to suppress the relaxation of the excited molecule, thus enhancing the fluorescence. On the other hand, the fluorescence quantum yields of the films containing **2** and **3** were both 16%. These values were lower due to the polarity of the carboxyl groups in PMMA, but the effect of polarity was smaller than in solution.

The photostability of **1** was measured in dichloromethane under UV light (370 nm) irradiation (Fig. 2d), similarly to other PyBTM derivatives.^{5,7,8,9,11} Since the emission of **2** and **3** was too weak to monitor in dichloromethane, the photostabilities of **2** and **3** were measured in cyclohexane (Fig. 2e).^{5,10} It should be noted that no decomposition of these radicals was observed in the dark. The half-lives (Table S7) indicated that **1** was 8–13 times more photostable than PyBTM in dichloromethane, while **2** and **3** were 6–9 times and 8–14 times more photostable than PyBTM in cyclohexane, respectively. The higher photostability of **3** than **2** indicates that the cationic methoxy groups generated by ICT may be vulnerable to nucleophilic attack in the excited state. In general, it has been reported that the addition of a donor on a radical improved the photostability of the radicals.^{2ef,3b,10,11,13d,15} Considering that the photostability of PyBTM was 71 times that of TTM in dichloromethane and 45 times that of TTM in cyclohexane, and that it was even comparable to closed-shell molecules with a long π -system such as TIPS pentacene,^{7a} the improved photostability of **1**, **2**, and **3** showed excellent values.

Conclusions

In summary, we synthesized novel photostable fluorescent radicals **1**, **2**, and **3** by attaching three or four phenyl groups to the *meta* and *para* positions of F₂PyBTM. By DFT calculation, their fluorescence is attributed to the radiation caused by the β -LUMO– β -HOMO electron transition, and the *o*-diphenylphenyl group works mainly as components of β -HOMO. Fluorescence brighter than that of the previous organic PyBTM derivatives in organic solvents, regardless of the polarity of the solvents, was observed for **1**. Electron-donating methoxy groups increased the polarization of the D₁ state, changing it from a locally excited state to an ICT state. The reorganization of the surrounding polar solvents then relaxed the excited state and quenched the fluorescence in the polar solvents. The fluorescence quantum yield of 19% of **2** in toluene was the highest among organic solvents. In polymer film, **1** showed a higher quantum yield of 33% in PMMA. Photostability, an advantage of introducing pyridyl groups, was further improved from PyBTM. Therefore, the luminescent materials produced in

this study are superior to PyBTM in both efficiency and durability, and will be useful for electroluminescent devices and a luminescent solar concentrator. The unique one-pot synthetic method of *meta*- and *para*-substitution is expected to produce other luminescent materials with photophysical advantages. In the future, we plan to develop a quadruple adduct of triarylmethyl radicals with higher fluorescence quantum yield and photostability.

Experimental

Materials and methods

The starting material, α H-*m*Br₂-F₂PyBTM was prepared according to the previous report.¹⁰ Commercially available compounds were used as received without further purification. Preparative recycling gel permeation chromatography was performed with a recycling preparative HPLC, LaboACE LC-5060, Japan Analytical Industry Co., Ltd. ¹H (400 MHz) and ¹³C NMR (100 MHz) spectra were recorded on a JEOL JNM-ECS 400 spectrometer using CDCl₃. The residual solvent signals (¹H NMR: δ 7.26, ¹³C NMR: δ 77.16) were used as the internal standards. ESR spectra were recorded with a JEOL JES-FR30EX spectrometer with X-band microwave. Sample solutions were charged in a 5 mm ϕ sample tube. Magnetic field was calibrated with the Mn²⁺/MgO standard. Mass spectrometry was performed with a JEOL-JMS-S3000 (MALDI-Spiral-TOF MS) mass spectrometer with DCTB (20 mg/mL in CHCl₃) as a matrix and TFANa (1 mg/mL in THF) as a cationization agent. Absorption and emission spectra were monitored on Hitachi U-4150 spectrophotometer and Hitachi F-7100 fluorescence spectrophotometer, respectively. Photostability under 370 nm light were recorded with a JASCO FP-8600KS spectrofluorometer. Absolute luminescence quantum yields were measured using Hamamatsu Photonics Quantaaurus QY. Photoluminescence decay curves were measured using a measurement system with a picosecond diode laser with the emission wavelength of 375 nm (Advanced Laser Diode Systems PIL037X) as light source, a single grating spectrometer (Andor Kymera193i-B1), and a photon counting detector (MPD SPD-050-CTE) operated with a time-correlated single photon counting (TCSPC) technique.

Synthesis of α H-Ph₄-F₂PyBTM (**1H**)

Water was carefully deoxygenated by bubbling N₂ under reflux for three hours, and Et₃N was carefully deoxygenated by freeze-pump-thaw degassing before use. In a 10 mL test tube equipped with a Schlenk-type adapter, α H-*m*Br₂-F₂PyBTM¹⁰ (171 mg, 0.267 mmol), phenylboronic acid (114 mg, 0.935 mmol), Pd(dtbpf)Cl₂ (6.96 mg, 0.0107 mmol), and Kolliphor EL (K-EL, 20 mg) were put under N₂ atmosphere. Deoxygenated water (1.0 mL) and toluene (0.11 mL) were added, and the mixture was vigorously stirred for 5 minutes. The mixture was therefore heated at 70 °C, and finally degassed Et₃N (0.26 mL, 1.9 mmol) was added. The reaction was maintained at 70 °C for four hours, checking the progress by TLC (eluent heptane/AcOEt 9:1), and finally cooled down to room temperature. The mixture was

extracted with AcOEt and the organic phase passed on a silica plug to collect the crude product in the form of an off-white powder. The crude product (136.6 mg) was separated by GPC (CHCl₃) to obtain pure **1H** (30.8 mg, 0.0426 mmol, 16%). A fraction including (3,5-difluoro-4-pyridyl)(2,6-dichloro-3,4-diphenyl)(3-phenyl-2,4,6-trichlorophenyl)methane (56.3 mg, ca. 85% purity by NMR) was obtained as a byproduct.

¹H NMR (400 MHz, CDCl₃, ppm): δ 8.36 (s, 1H), 8.25 (s, 1H), 7.39 (s, 2H), 7.25-7.18 (m, 6H), 7.18-7.12 (m, 6H), 7.12-7.01 (m, 9H).

¹³C NMR (100 MHz, CDCl₃, ppm): δ 143.1, 139.4, 138.2, 136.6, 133.5, 130.8, 130.7, 129.6, 127.9, 127.4, 127.3, 120.1, 43.9.

HRMS (MALDI-TOF MS) m/z:[M]⁺ Calcd for C₄₂H₂₆Cl₄F₂N⁺ 722.07819; Found 722.07824.

Synthesis of αH-(MeOPh)₄-F₂PyBTM (**2H**) and αH-(MeOPh)₃-F₂PyBTM (**3H**)

Water was carefully deoxygenated by bubbling N₂ under reflux for three hours, and Et₃N was carefully deoxygenated by freeze-pump-thaw degassing before use. In a 10 mL test tube equipped with a Schlenk-type adapter, αH-*m*Br₂-F₂PyBTM¹⁰ (136 mg, 0.211 mmol), 4-methoxyphenylboronic acid (138 mg, 0.908 mmol), Pd(dtbpf)Cl₂ (5.50 mg, 0.0844 mmol), and Kolliphor EL (K-EL, 16 mg) were put under N₂ atmosphere. Deoxygenated water (0.80 mL) and toluene (0.09 mL) were added, and the mixture was vigorously stirred for 5 minutes. The mixture was therefore heated at 70 °C, and finally degassed Et₃N (0.28 mL, 1.8 mmol) was added. The reaction was maintained at 70 °C for 16 hours, checking the progress by TLC (eluent heptane/AcOEt 8:2), and finally cooled down to room temperature. The mixture was extracted with AcOEt and the organic phase passed on a silica plug to collect the crude product in the form of an off-white powder. The crude product (156.3 mg) was separated by GPC (CHCl₃) to obtain pure **2H** (20.6 mg, 0.0244 mmol, 12%) and **3H** (64.5 mg, 0.0836 mmol, 40%). From another reaction, **3H** could be also separated by chromatography using heptane/AcOEt 8:2 as eluent.

2H

¹H NMR (400 MHz, CDCl₃, ppm): δ 8.34 (s, 1H), 8.23 (s, 1H), 7.35 (s, 2H) 7.03-3.92 (m, 9H), 6.82-6.73 (m, 4H), 6.73-6.67 (m, 4H), 3.77 (s, 6H), 3.75 (s, 6H).

¹³C NMR (100 MHz, CDCl₃, ppm): δ 158.7, 142.9, 137.0, 135.2, 135.1, 135.0, 133.4, 133.1, 132.0, 131.9, 130.8, 130.7, 113.4, 55.3, 44.0.

HRMS (MALDI-TOF MS) m/z:[M]⁺ Calcd for C₄₆H₃₃Cl₄F₂NO₄⁺ 841.11263; Found 841.11245.

3H

¹H NMR (400 MHz, CDCl₃, ppm): δ 8.34 (s, 1H), 8.23 (s, 1H), 7.48 (s, 1H), 7.35 (s, 1H), 7.18-7.08 (m, 2H), 7.02-6.92 (m, 6H), 6.90 (s, 1H), 6.80-6.73 (m, 2H), 6.72-6.67 (m, 2H).

¹³C NMR (100 MHz, CDCl₃, ppm): δ 159.5, 158.8, 143.1, 139.3, 137.8, 136.9, 135.7, 135.6, 135.3, 135.0, 134.7, 133.7, 133.5, 132.5, 131.9, 131.8, 130.8, 130.6, 129.9, 129.8, 125.3, 125.1, 125.0, 113.8, 113.4, 55.3, 43.8.

HRMS (MALDI-TOF MS) m/z:[M]⁺ Calcd for C₃₉H₂₆Cl₅F₂NO₃⁺ 769.03179; Found 769.03184.

Synthesis of Ph₄-F₂PyBTM (**1**)

Under an argon atmosphere, αH-Ph₄-F₂PyBTM (**1H**, 30.6 mg, 0.0423 mmol) was dissolved in dry THF (~3 mL), and *t*BuOK in THF (1M solution, 0.15 mL, 3.5 eq.) was added. The reaction mixture was stirred overnight in the dark. I₂ (70.5 mg, 0.278 mmol, 6.6 eq.) in dry THF was added and stirred for 2.5 h. The reaction mixture was quenched with Na₂S₂O₃ aq, brine was added, and extracted with Et₂O. The organic layer was dried with Na₂SO₄, filtered, evaporated, purified by flash chromatography on silica gel (CHCl₃: hexane = 1: 2→1: 1) and dried in vacuo to afford **1** (29.7 mg, 0.0411 mmol, 97%) as a dark red solid.

HRMS (MALDI-TOF MS) m/z:[M]⁺ Calcd for C₄₂H₂₄Cl₄F₂N⁺ 720.06254; Found 720.06227.

Synthesis of (MeOPh)₄-F₂PyBTM (**2**)

Under an argon atmosphere, αH-(MeOPh)₄-F₂PyBTM (**2H**, 20.6 mg, 0.0244 mmol) was dissolved in dry THF (~3 mL), and *t*BuOK in THF (1 M solution, 0.1 mL, 4.1 eq.) was added. The reaction mixture was stirred overnight in the dark. Because the amount of **2H** was small, we used silver nitrate as an oxidant to avoid yield of byproducts from iodination of the methoxyphenyl rings.¹⁰ Silver nitrate (27.4 mg, 0.16 mmol) in acetonitrile (0.6 mL) was added and stirred for 1 h. The reaction mixture was purified by Al₂O₃ column chromatography with CHCl₃ and dried in vacuo to afford **2** (19.2 mg, 0.0228 mmol, 93%) as a black solid.

HRMS (MALDI-TOF MS) m/z:[M]⁺ Calcd for C₄₆H₃₂Cl₄F₂NO₄⁺ 840.10480; Found 841.10429.

Synthesis of (MeOPh)₃-F₂PyBTM (**3**)

Under nitrogen atmosphere, αH-(MeOPh)₃-F₂PyBTM (**3H**, 77.1 mg, 0.0100 mmol) was dissolved in dry THF (1.5 mL), and *t*BuOK (39.3 mg, 0.350 mmol) in THF (1.5 mL) was added. The reaction mixture was stirred for 4.5 hours in the dark. Iodine (147 mg, 0.579 mmol) in THF (1.5 mL) was added and stirred for 2 h. The reaction mixture was quenched with aqueous NaHSO₃ and extracted with Et₂O. The organic layer was dried with Na₂SO₄, filtered, evaporated, purified by flash chromatography on silica gel (CH₂Cl₂:Et₂O 4:1) and dried in vacuo to afford **3** (25.0 mg, 0.0324 mmol, 32%) as a black solid.

HRMS (MALDI-TOF MS) m/z:[M]⁺ Calcd for C₃₉H₂₅Cl₅F₂NO₃⁺ 768.02397; Found 768.02450.

Author Contributions

S. M., Y. H., T. K. and L. B. conceived the project. R. K. prepared αH-*m*Br₂-F₂PyBTM. S. M. synthesized **1H**, **2H**, **3H** and **3**. Y. H., R. K. and R. M. prepared **1** and **2**. Y. H. carried out measurements and DFT calculations. S. M. and Y. H. wrote original draft, and R. M., T. K., K. U. and L. B. reviewed and edited.

Conflicts of interest

There are no conflicts to declare.

Acknowledgements

We thank Prof. Takehiro Kawauchi, Ryukoku University for absolute luminescence quantum yield measurements. We acknowledge support by Ms. Yoshiko Nishikawa and Ms. Mieko Yamagaki for HRMS (MALDI-TOF MS) conducted in NAIST. This work was supported by Nanotechnology Platform Program <Molecules and Material Synthesis> of the Ministry of Education, Culture, Sports, Science and Technology (MEXT), Japan., Grant Number JPMXP09S21NR0009. We gratefully acknowledge the financial contribution from MIUR under Grant PRIN2017 BOOSTER (2017YXX8AZ), Cooperative Research by Institute for Molecular Science (IMS program 22IMS1222), CREST program grant JPMJCR17N2 of the Japan Science and Technology Agency, and JSPS KAKENHI Grant Number JP20H02759.

Notes and references

- 1 a) S. Dong and Z. Li, *J. Mater. Chem. C*, 2022, **10**, 2431–2449; b) P. Murto and H. Bronstein, *J. Mater. Chem. C*, 2022, **10**, 7368–7403; c) R. Matsuoka, A. Mizuno, T. Mibu and T. Kusamoto, *Coord. Chem. Rev.*, 2022, **467**, 214646.
- 2 a) H. Namai, H. Ikeda, Y. Hoshi, N. Kato, Y. Morishita and K. Mizuno, *J. Am. Chem. Soc.*, 2007, **129**, 9032–9036; b) Q. Peng, A. Obolda, M. Zhang and F. Li, *Angew. Chem. Int. Ed.*, 2015, **54**, 7091–7095; c) X. Ai, E. W. Evans, S. Dong, A. J. Gillett, H. Guo, Y. Chen, T. J. H. Hele, R. H. Friend and F. Li, *Nature*, 2018, **563**, 536–540; d) Y. Beldjoudi, M. A. Nascimento, Y. J. Cho, H. Yu, H. Aziz, D. Tonouchi, K. Eguchi, M. M. Matsushita, K. Awaga, I. Osorio-Roman, C. P. Constantinides and J. M. Rawson, *J. Am. Chem. Soc.*, 2018, **140**, 6260–6270; e) H. Guo, Q. Peng, X.-K. Chen, Q. Gu, S. Dong, E. W. Evans, A. J. Gillett, X. Ai, M. Zhang, D. Credgington, V. Coropceanu, R. H. Friend, J.-L. Brédas and F. Li, *Nat. Mater.*, 2019, **18**, 977–984; f) A. Abdurahman, T. J. H. Hele, Q. Gu, J. Zhang, Q. Peng, M. Zhang, R. H. Friend, F. Li and E. W. Evans, *Nat. Mater.*, 2020, **19**, 1224–1229.
- 3 a) Y. Hattori, S. Kimura, T. Kusamoto, H. Maeda and H. Nishihara, *Chem. Commun.*, 2018, **54**, 615–618; b) C.-H. Liu, E. Hamzehpoor, Y. Sakai-Otsuka, T. Jadhav and D. F. Perepichka, *Angew. Chem. Int. Ed.*, 2020, **59**, 23030–23034.
- 4 a) S. Kimura, T. Kusamoto, S. Kimura, K. Kato, Y. Teki and H. Nishihara, *Angew. Chem. Int. Ed.*, 2018, **57**, 12711–12715; b) K. Kato, S. Kimura, T. Kusamoto, H. Nishihara and Y. Teki, *Angew. Chem. Int. Ed.*, 2019, **58**, 2606–2611; c) S. Kimura, S. Kimura, K. Kato, Y. Teki, H. Nishihara and T. Kusamoto, *Chem. Sci.*, 2021, **12**, 2025–2029; d) S. Kimura and T. Kusamoto, *Chem. Lett.*, 2021, **50**, 1445–1459.
- 5 Y. Hattori, T. Kusamoto and H. Nishihara, *Angew. Chem. Int. Ed.*, 2014, **53**, 11845–11848.
- 6 O. Armet, J. Veciana, C. Rovira, J. Riera, J. Casteñer, E. Molins, J. Rius, C. Miravittles, S. Olivella and J. Brichfeus, *J. Phys. Chem.*, 1987, **91**, 5608–5616.
- 7 a) S. Kimura, A. Tanushi, T. Kusamoto, S. Kochi, T. Sato and H. Nishihara, *Chem. Sci.*, 2018, **9**, 1996–2007; b) S. Kimura, M. Uejima, W. Ota, T. Sato, S. Kusaka, R. Matsuda, H. Nishihara and T. Kusamoto, *J. Am. Chem. Soc.*, 2021, **143**, 4329–4348.
- 8 a) Y. Hattori, T. Kusamoto and H. Nishihara, *Angew. Chem. Int. Ed.*, 2015, **54**, 3731–3734; b) Y. Hattori, T. Kusamoto, T. Sato and H. Nishihara, *Chem. Commun.*, 2016, **52**, 13393–13396; c) Y. Hattori, R. Kitajima, R. Matsuoka, T. Kusamoto, H. Nishihara and K. Uchida, *Chem. Commun.*, 2022, **58**, 2560–2563.
- 9 Y. Hattori, T. Kusamoto and H. Nishihara, *RSC Adv.*, 2015, **5**, 64802–64805.
- 10 Y. Hattori, S. Tsubaki, R. Matsuoka, T. Kusamoto, H. Nishihara and K. Uchida, *Chem. Asian J.*, 2021, **16**, 2538–2544.
- 11 S. Mattiello, F. Corsini, S. Mecca, M. Sassi, R. Ruffo, G. Mattioli, Y. Hattori, T. Kusamoto, G. Griffini and L. Beverina, *Mater. Adv.*, 2021, **2**, 7369–7378.
- 12 a) S. Handa, Y. Wang, F. Gallou and B. H. Lipshutz, *Science*, 2015, **349**, 1087–1091; b) S. Mattiello, M. Rooney, A. Sanzone, P. Brazzo, M. Sassi and L. Beverina, *Org. Lett.*, 2017, **19**, 654–657; c) M. Rooney, S. Mattiello, R. Stara, A. Sanzone, P. Brazzo, M. Sassi and L. Beverina, *Dyes Pigm.*, 2018, **149**, 893–901.
- 13 a) V. Gamero, D. Velasco, S. Latorre, F. López-Calahorra, E. Brillas and L. Juliá, *Tetrahedron Lett.* 2006, **47**, 2305–2309; b) D. Velasco, S. Castellanos, M. López, F. López-Calahorra, E. Brillas and L. Juliá, *J. Org. Chem.*, 2007, **72**, 7523–7532; c) S. Castellanos, D. Velasco, F. López-Calahorra, E. Brillas and L. Juliá, *J. Org. Chem.*, 2008, **73**, 3759–3767; d) S. Dong, W. Xu, H. Guo, W. Yan, M. Zhang and F. Li, *Phys. Chem. Chem. Phys.*, 2018, **20**, 18657–18662.
- 14 A. Heckmann, S. Dümmler, J. Pauli, M. Margraf, J. Köhler, D. Stich, C. Lambert, I. Fischer and U. Resch-Genger, *J. Phys. Chem. C*, 2009, **113**, 20958–20966.
- 15 a) Y. C. Gao, W. Xu, H. W. Ma, A. Obolda, W. F. Yan, S. Z. Dong, M. Zhang and F. Li, *Chem. Mater.*, 2017, **29**, 6733–6739; b) Y. Zhao, A. Abdurahman, Y. Zhang, P. Zhang, M. Zhang and F. Li, *CCS Chem.*, 2022, **4**, 722–731.
- 16 S. Sang, F. Chen and C. Zhang, *Int. J. Quantum Chem.*, 2021, **121**, e26522.
- 17 M. Ito, S. Shirai, Y. Xie, T. Kushida, N. Ando, H. Soutome, K. J. Fujimoto, T. Yanai, K. Tabata, Y. Miyata, H. Kita and S. Yamaguchi, *Angew. Chem. Int. Ed.*, 2022, e202201965.
- 18 a) M. López, D. Velasco, F. López-Calahorra and L. Juliá, *Tetrahedron Lett.*, 2008, **49**, 2196–5199; b) L. Fajari, R. Papoular, M. Reig, E. Brillas, J. L. Jorda, O. Vallcorba, J. Rius, D. Velasco and L. Juliá, *J. Org. Chem.*, 2014, **79**, 1771–1777; c) Y. Hattori, E. Michail, A. Schmiedel, M. Moos, M. Holzappel, I. Krummenacher, H. Braunschweig, U. Meller, J. Pflaum and C. Lambert, *Chem. Eur. J.*, 2019, **25**, 15463–15471.
- 19 E. Cho, V. Coropceanu, J.-L. Brédas and F. Li, *J. Am. Chem. Soc.*, 2020, **142**, 17782–17786.